K. J. A. Franke, P. R. Dean, M. Ciomaga Hatnean (iD), M. T. Birch, D. D. Khalyavin, P. Manuel, T. Lancaster (iD), G. Balakrishnan, and P. D. Hatton

COLLECTIONS

View Online   Export Citation   CrossMark

ARTICLES YOU MAY BE INTERESTED IN

Perspective: Magnetic skyrmions—Overview of recent progress in an active research field
Journal of Applied Physics **124**, 240901 (2018); https://doi.org/10.1063/1.5048972

Large topological Hall effect in a geometrically frustrated kagome magnet Fe$_3$Sn$_2$
Applied Physics Letters **114**, 192408 (2019); https://doi.org/10.1063/1.5088173

Voltage-controlled superconducting magnetic memory
AIP Advances **9**, 125223 (2019); https://doi.org/10.1063/1.5129135

Investigating the magnetic ground state of the skyrmion host material Cu₂OSeO₃ using long-wavelength neutron diffraction

K. J. A. Franke,[1,2,3,a)] P. R. Dean,[1] M. Ciomaga Hatnean,[4] M. T. Birch,[1] D. D. Khalyavin,[5] P. Manuel,[5] T. Lancaster,[1] G. Balakrishnan,[4] and P. D. Hatton[1,b)]

AFFILIATIONS

[1] Centre for Materials Physics, Durham University, Durham DH1 3LE, United Kingdom
[2] School of Physics and Astronomy, University of Leeds, Leeds LS2 9JT, United Kingdom
[3] Department of Materials Science and Engineering, University of California, Berkeley, Berkeley, California 94720, USA
[4] University of Warwick, Department of Physics, Coventry CV4 7AL, United Kingdom
[5] ISIS Facility, STFC Rutherford Appleton Laboratory, Chilton, Didcot, Oxfordshire OX11 0QX, United Kingdom

Note: This paper was presented at the 64th Annual Conference on Magnetism and Magnetic Materials.
a) Corresponding Author. Electronic mail: K.J.A.Franke@leeds.ac.uk
b) Electronic mail: p.d.hatton@durham.ac.uk

ABSTRACT

We present long-wavelength neutron diffraction data measured on both single crystal and polycrystalline samples of the skyrmion host material Cu₂OSeO₃. We observe magnetic satellites around the $(0\bar{1}1)$ diffraction peak not accessible to other techniques, and distinguish helical from conical spin textures in reciprocal space. Our measurements show that not only the field-polarised phase but also the helical ground state are made up of ferrimagnetic clusters instead of individual spins. These clusters are distorted Cu tetrahedra, where the spin on one Cu ion is anti-aligned with the spin on the three other Cu ions.

I. INTRODUCTION

Skyrmions are topologically protected, nano-sized swirls of spins found in a range of magnetic materials. The phase diagram of Cu₂OSeO₃ resembles that of other skyrmion hosting systems such as several B20 compounds, or β-Mn-type CoZnMn alloys.[1–5] Competition between the symmetric exchange interaction promoting parallel alignment of spins and the antisymmetric Dzyaloshinskii-Moriya interaction (DMI)[6,7] leads to a magnetic ground state that consists of helices, long period magnetic structures where the magnetisation rotates in a plane perpendicular to the propagation direction. Previous investigations have either shown that Cu₂OSeO₃ is a ferrimagnet[8–10] without addressing the chiral nature of the magnetic ground state, or investigated the chirality without taking into account ferrimagnetism.[4,11–14]

Here we investigate the magnetic microstructure of the magnetic phases of Cu₂OSeO₃ and address the question of whether the ground state helical (H) structure is also ferrimagnetic. Using time-of-flight long-wavelength neutron diffraction on a single crystal sample, we observe magnetic satellites around the $(0\bar{1}1)$ diffraction peak not accessible to other techniques. Furthermore, our measurements uniquely allow us to distinguish H from conical (C) spin textures in reciprocal space. We show successive transitions from H to C to field-polarised (FP) as the external magnetic field is increased in the magnetically ordered phases, and the formation of a skyrmion lattice with propagation vectors perpendicular to the field direction in a region of the field-temperature phase diagram that is consistent with previous reports.[4,11] We use powder diffraction measurements to determine the magnetic microstructure of the FP and H phases, and show that not only the FP phase but also the H ground

state are made up of ferrimagnetic clusters instead of individual spins.

II. METHODS

Polycrystalline samples of Cu_2OSeO_3 were synthesized as described previously.[9] The same polycrystalline powder was also used for the growth of single crystals by the chemical vapour transport technique following the procedure described in Ref. 4.

DC magnetisation measurements were performed using SQUID magnetometry, in a Quantum Design MPMS. AC susceptibility measurements were performed on the same instrument at an excitation frequency of 10 Hz with an amplitude of 0.1 mT.

Neutron powder and single crystal diffraction experiments were performed on the time-of-flight long-wavelength neutron diffractometer WISH[15] at the ISIS Facility of the Rutherford Appleton Laboratory (UK) to determine the crystal and magnetic structures. The WISH detector system consists of pixelated ^3He gas tubes covering scattering angles from $2\Theta = 10°$ to $2\Theta = 170°$ in the plane and $\pm 12.8°$ out of the plane. Powder diffraction patterns are measured at fixed scattering angles 2Θ as a function of the time-of-flight (which is related to d-spacing). The highest resolution is offered at large scattering angles which require longer wavelength neutrons. This, however, limits the highest observable d-spacing. For measuring powder diffraction patterns, we thus consider two detector banks, at $2\Theta = 27°$ and $2\Theta = 58°$. For single crystal diffraction patterns we restricted the neutron wavelength to 8.2 ± 0.2 Å to observe the $(0\bar{1}1)$ Bragg peak and its magnetic satellites.

Data reduction, analysis, and simulation of single crystal diffraction patterns was done using the Mantid software.[16] Rietveld refinement of powder diffraction data was undertaken using the FullProf suite of programs.[17]

III. RESULTS AND DISCUSSION

A. Magnetisation

AC susceptibility measurements have proven powerful in determining the presence and location of the SL.[18,19] Figure 1(a) shows the real part χ' of the AC susceptibility from measurements on Cu_2OSeO_3 with the magnetic field μ_0H applied along the [111]

direction. The SL is identified as a decrease in χ' relative to the surrounding C phase. It is located in the range $12 \leq \mu_0H \leq 30$ mT and $55.75 \leq T \leq 58$ K in agreement with previous observations.[4,11]

The inverse (DC) susceptibility $1/\chi$ presented in Figure 1(b) confirms a critical temperature $T_c \approx 59$ K. Above T_c, however, the temperature dependence of $1/\chi$ does not agree with the earlier report by Bos et al.:[9] in the PM phase, we observe a negative curvature (noted in an early paper by Kohn[8]), instead of a linear increase with temperature as observed for ferromagnets and antiferromagnets. This dependence is characteristic of ferrimagnets,[20] and is particularly clear with the log-log scale used here. Magnetisation measurements in the PM phase thus indicate a ferrimagnetic alignment of spins.

B. Single crystal diffraction

For single crystal diffraction the sample was also mounted with the applied field along the [111] direction. Data measured around the $(0\bar{1}1)$ Bragg peak (yellow dot) is presented in Figure 2. The structural peak is removed by subtracting the structural diffraction pattern measured in zero field in the PM phase, thus showing only magnetic peaks. The technique is distinct from SANS, where the scattering around the transmitted neutron beam is investigated. The operating principle of our single crystal neutron diffraction is more similar to resonant elastic x-ray scattering,[21,22] in that periodically modulated spin textures are observed as satellite peaks around a structural Bragg reflection. As resonant elastic x-ray scattering relies on matching the photon energy (and thus wavelength) to a x-ray absorption edge, only the (001) peak of Cu_2OSeO_3 is accessible at the Cu L_3 edge (in many other skyrmion hosts, such as FeGe or MnSi, no Bragg peaks are accessible at all).[22] Single crystal neutron diffraction has the advantage of allowing access to a wide range of structural diffraction peaks, such as the $(0\bar{1}1)$ peak considered here. It furthermore allows distinguishing helices and cones as detailed below.

At 50 K, in the absence of an applied magnetic field [Fig. 2(a)], satellite peaks (green dots) oriented along {100} directions are observed as expected in the H phase:[11,12] Two peaks observed to the left and right of the Bragg peak correspond to the (100) direction. Two peaks above and below the Bragg peak correspond to the (010) and (001) directions (these satellites coincide due to the orientation of the sample in the instrument). We extract a helical
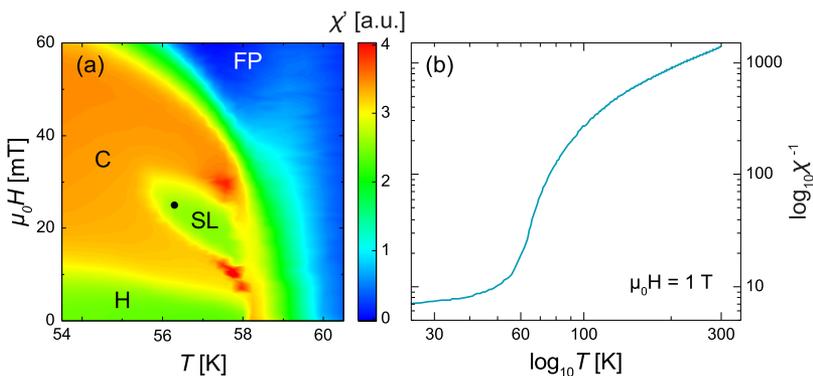

FIG. 1. (a) AC susceptibility mapping of the phase diagram of Cu_2OSeO_3 for H ∥ [111]. The black dot indicates where the single crystal diffraction data in Figure 2(e) was measured. (b) Inverse susceptibility as a function of temperature.
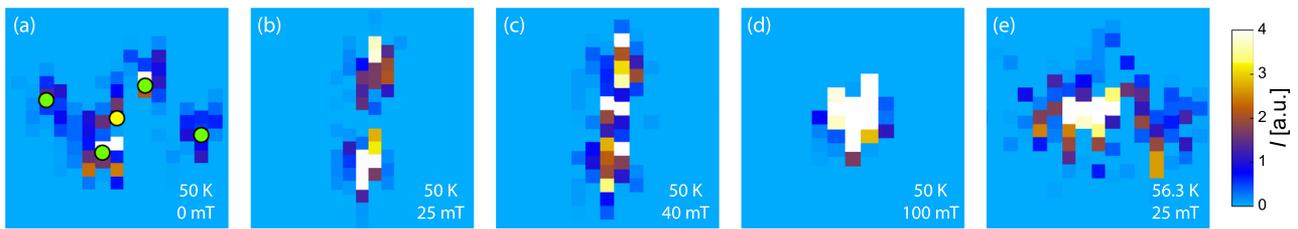
FIG. 2. (a)-(d) Magnetic contribution to single crystal neutron diffraction data measured around the $(0\bar{1}1)$ Bragg peak (yellow dot) at 50 K as a function of increasing applied magnetic field. Green dot are fits to the helical peaks. (e) Measurement in the SL phase [c.f. black dot in Figure 1(a)].

Q of 0.0016(3) Å^{-1}, in agreement with previous SANS measurements.[11,12] Upon the application of a magnetic field ($\mu_0 H$ = 25 mT), the helices rotate towards the field direction [Fig. 2(b)]. No central peak is observed indicating the absence of a net magnetic moment as expected for a helix. A further increase of the magnetic field to $\mu_0 H$ = 40 mT [Fig. 2(c)] induces a spin canting and the structure becomes conical. This is observed as the appearance of intensity at the parent peak position, indicating a net magnetic moment. When the applied field is increased further [Fig. 2(d)], all moments align with the field ($\mu_0 H$ = 100 mT). Figure 2(e) shows the diffraction pattern measured at 56.3 K in 25 mT, at the location of the skyrmion phase [c.f. black dot in Figure 1(a)]. The resolution is too low to distinguish separate peaks, but a transfer of intensity from aligned along the applied field direction to the plane perpendicular to the field is observed, showing that the propagation vectors of the skyrmion lattice are in a plane perpendicular to the applied field. The scattering plane is perpendicular to the applied field direction, and SL satellites are thus expected along a (horizontal) line in Figure 2(e). The lack of magnetic satellites above and below the parent Bragg peak precludes the coexistence of the skyrmion phase with the C phase in our sample.

The resolution of our single crystal diffraction data is not sufficient to easily distinguish the 6-fold SL satellites. However, our measurements shows that the magnetic phase can be transformed from H to FP via the C phase by an increase in the applied magnetic field $\mu_0 H$, and to the SL phase by a change in temperature. Single crystal neutron diffraction measurements agree with the phase diagram established by AC susceptibility measurements and the helical wavelength established in SANS measurements.[11,12]

C. Powder diffraction

Neutron powder diffraction data measured at 60 K in the PM phase is partially shown in Figure 4(a). The pattern was measured at zero magnetic field and thus contains only structural information. The crystallographic parameters obtained from Rietveld refinement are best fitted to the space group $P2_1 3$ with lattice parameter a = 8.97639(7) Å in agreement with previous reports.[9] The crystal structure of Cu_2OSeO_3 is shown in Figure 3(a). The sixteen Cu ions in the unit cell sit on two different Wyckoff sites, four Cu1 ions on the 4a and twelve Cu2 ions on the 12b site. Cu1 ions bond with oxygen ions to form bipyramidal CuO_5 units, while Cu2 ions are bonded in distorted square based CuO_5 pyramids. The Cu^{2+} ions are arranged in a network of distorted tetrahedra consisting of one Cu1 and three Cu2 ions.

Data measured in the FP phase at 20 K in an applied field $\mu_0 H$ = 120 mT is shown in Figure 4(a). Analogous to our approach for single crystal diffraction, the difference ΔI between patterns in the FP and the PM phases is shown in Figure 4(b). ΔI should contain purely magnetic information, however, thermal contraction can lead to a small shift of structural peaks between the data measured at 60 K and 20 K. This can be identified by the shape of the difference peaks as a negative peak next to a positive peak (a shape resembling the derivative of a δ-function). This is for example observed at the (111) reflection in Figure 4(b). Clear magnetic contributions to the diffraction pattern are observed at the (110) and (201) reflections. The data is best fitted with a model with spins on Cu1 ions aligned antiparallel to the spins on Cu2 ions, as sketched in Figure 3(d), and a magnetic moment of 0.92(3) μ_B for each Cu ion. The FP phase is thus
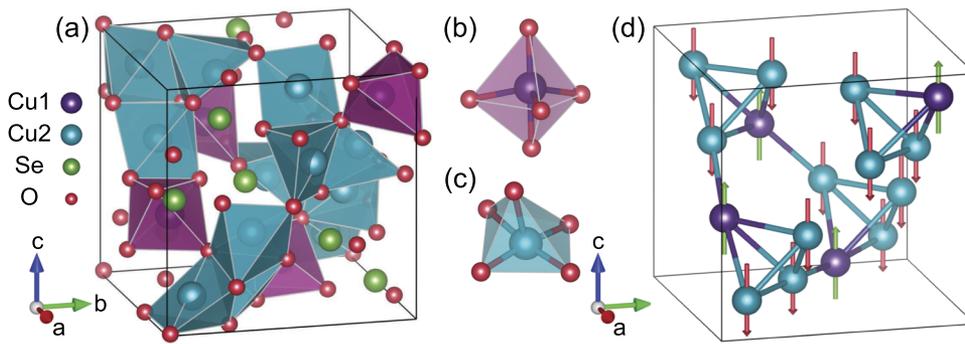

FIG. 3. (a) Crystal structure of Cu_2OSeO_3 consisting of (b) Cu1 bipyramids and (c) Cu2 distorted square based pyramids. Bonds to Se ions have been omitted for clarity. (d) Representation of the ferrimagnetic structure with spins (green arrows) on Cu1 site antiparallel to the spins (red arrows) on Cu2 sites.
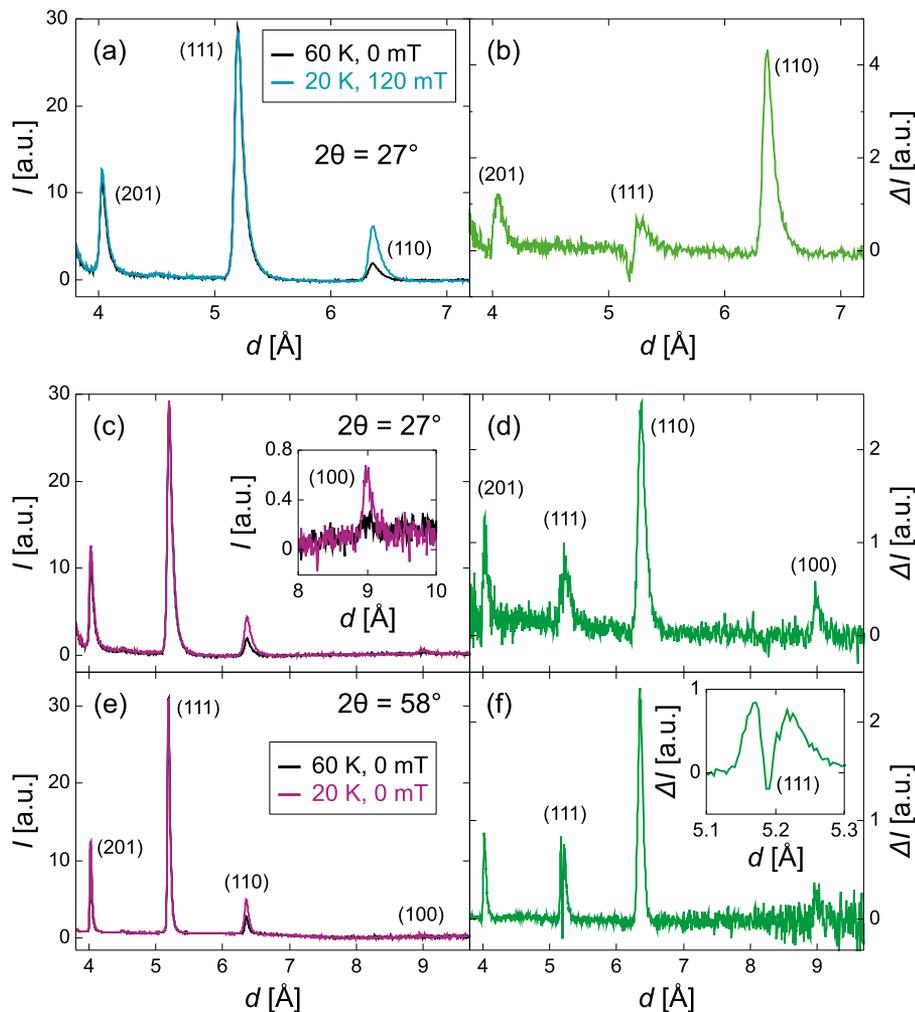
FIG. 4. (a) Neutron powder diffraction data measured in the FP (blue) and PM (black) phases at a scattering angles of $2\Theta = 27°$. (b) Difference between both patterns. (c) & (e) Data measured in the H (violet) and PM (black) phases at scattering angles of $2\Theta = 27°$ and $2\Theta = 58°$. The difference between H and PM phases is shown in (d) and (f).

ferrimagnetic, consisting of clusters of four Cu ions, where the spin on one Cu1 ion is anti-aligned with the spins on three Cu2 ions.

The H phase was investigated at 20 K in zero field. The data measured at $2\Theta = 27°$ and $2\Theta = 58°$ is again compared to the data measured in the PM phase in Figures 4(c)–4(f). In addition to the magnetic (110) peak already observed in the ferrimagnetic phase, additional purely magnetic peaks are observed at the (100) position [as highlighted in the inset of Figure 4(c)] and the (111) position. The higher resolution data at $2\Theta = 58°$ reveals the latter to be due to the presence of two magnetic satellite peaks, as shown in the inset of Figure 4(f). As for the single crystal diffraction data, the presence of these satellites around a structural Bragg reflection indicates the presence of a long-range periodically modulated spin texture. The data in the H phase was best fitted by a helical model, where the relative orientation of spins within the unit cell is fixed, but helically modulated between unit cells with a Q of 0.0015 Å^{-1}. This corresponds to a helical state consisting of ferrimagnetic clusters, where we fit an average moment size of $0.74(4)$ μ_B/Cu, and thus lower than the moment in the ferrimagnetic phase.

We attribute this to the degenerate ground state, where the helical wavevector can point in any {100} direction. Fluctuations can thus lead to a reduction in the observed magnetic moment. The magnetic peak at the (100) position is forbidden for both ferromagnetic and ferrimagnetic order and may indicate local canting of spins in addition to the helical ground state as predicted by Chizhikov and Dmitrienko.[23,24]

While neutron powder diffraction patterns can be fitted by Rietveld refinement, a qualitative analysis is instructive in understanding the helical ground state of Cu_2OSeO_3. To that end Figure 5 presents simulated powder diffraction patterns for (a) helices composed of individual spins, and (c) helices with ferrimagnetic alignment of spins within Cu tetrahedra. An exaggerated magnetic moment (4 μ_B/Cu) and Q (0.08 Å^{-1}) have been used to better distinguish helical satellite peaks. Simulations reproducing the PM phase are included for comparison and the difference between patterns shown in Figures 5(b) and (d). Both models predict the absence of a magnetic (111) peak, but the presence of magnetic satellites around it. They furthermore show a magnetic peak and
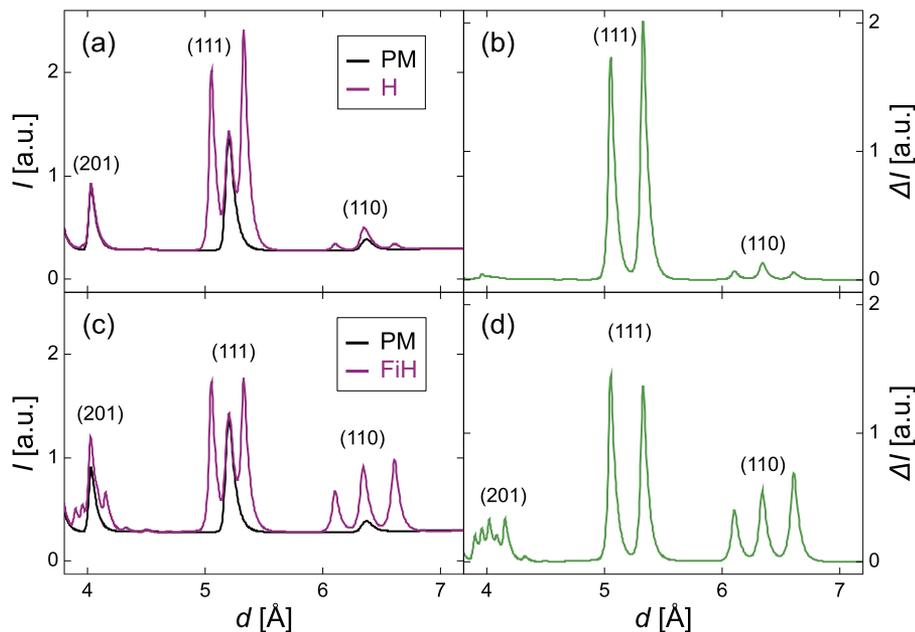
FIG. 5. Simulations for powder patterns with exaggerated magnetic moments and helical wavevector of the PM (black lines) and H (violet) phases of Cu_2OSeO_3 for (a) helices made from individual spins, and (c) helices composed of ferrimagnetic clusters. The difference between simulated H and PM diffraction patterns are displayed in (b) and (d).

satellites at (110). However these are more pronounced in the ferrimagnetic model. Finally, only the ferrimagnetic model indicates a magnetic peak at the (201) Bragg peak position. Comparing the neutron diffraction data presented in Figure 4 with the simulations in Figure 5 it becomes apparent that the magnetic ground state of Cu_2OSeO_3 does not only consist of helices, but that these are made up of ferrimagnetically aligned clusters of spins: the H satellites predicted around the structural (111) peak are clearly observed in Figure 4(f). Magnetic satellites are not resolved around the (110) peak in the diffraction measurements, but a large magnetic peak is most likely consistent with the ferrimagnetic cluster model of the H phase. Finally, the magnetic peak observed at the (201) position is only accounted for by the ferrimagnetic cluster model. We have thus established the magnetic ground state of Cu_2OSeO_3 to be composed of helices made from ferrimagnetically aligned spin clusters instead of individual spins.

IV. CONCLUSION

Single crystal and powder long-wavelength neutron diffraction data was measured on the skyrmion host Cu_2OSeO_3. We observe magnetic satellites around the $(0\bar{1}1)$ diffraction peak not accessible by other techniques, and distinguish helical from conical spin textures in reciprocal space. Measurements show successive transitions from a helical to a conical to a field-polarised magnetic phase as the external magnetic field is increased. While the resolution is too low to resolve the individual 6-fold skyrmion satellites, the formation of a skyrmion lattice with propagation vectors perpendicular to the field direction is observed. As our key result, we show that not only the field-polarised phase but also the helical ground state are made up of ferrimagnetic clusters instead of individual spins. These clusters are distorted Cu tetrahedra, where the spin on the Cu1 ion is anti-aligned with the spin on three Cu2 ions.

Supporting magnetometry in the paramagnetic phase confirms the proposed ferrimagnetism.

REFERENCES

[1] S. Mühlbauer, B. Binz, F. Jonietz, C. Pfleiderer, A. Rosch, A. Neubauer, R. Georgii, and P. Böni, "Skyrmion lattice in a chiral magnet," Science **323**, 915–919 (2009).

[2] X. Z. Yu, Y. Onose, N. Kanazawa, J. H. Park, J. H. Han, Y. Matsui, N. Nagaosa, and Y. Tokura, "Real-space observation of a two-dimensional skyrmion crystal," Nature **465**, 901–904 (2010).

[3] X. Z. Yu, N. Kanazawa, Y. Onose, K. Kimoto, W. Z. Zhang, S. Ishiwata, Y. Matsui, and Y. Tokura, "Near room-temperature formation of a skyrmion crystal in thin-films of the helimagnet FeGe," Nat. Mater. **10**, 106–109 (2011).

[4] S. Seki, X. Z. Yu, S. Ishiwata, and Y. Tokura, "Observation of skyrmions in a multiferroic material," Science **336**, 198–201 (2012).

[5] Y. Tokunaga, X. Z. Yu, J. S. White, H. M. Rønnow, D. Morikawa, Y. Taguchi, and Y. Tokura, "A new class of chiral materials hosting magnetic skyrmions beyond room temperature," Nat. Commun. **6**, ncomms8638 (2015).

[6] I. Dzyaloshinsky, "A thermodynamic theory of "weak" ferromagnetism of antiferromagnetics," J. Phys. Chem. Solids **4**, 241–255 (1958).

[7] T. Moriya, "Anisotropic superexchange interaction and weak ferromagnetism," Phys. Rev. **120**, 91–98 (1960).

[8] K. Kohn, "A new ferrimagnet Cu_2SeO_4," J. Phys. Soc. Jpn. **42**, 2065–2066 (1977).

[9] J.-W. G. Bos, C. V. Colin, and T. T. M. Palstra, "Magnetoelectric coupling in the cubic ferrimagnet Cu_2OSeO_3," Phys. Rev. B **78**, 094416 (2008).

[10] M. Belesi, I. Rousochatzakis, H. C. Wu, H. Berger, I. V. Shvets, F. Mila, and J. P. Ansermet, "Ferrimagnetism of the magnetoelectric compound Cu_2OSeO_3 probed by ^{77}Se NMR," Phys. Rev. B **82**, 094422 (2010).

[11] T. Adams, A. Chacon, M. Wagner, A. Bauer, G. Brandl, B. Pedersen, H. Berger, P. Lemmens, and C. Pfleiderer, "Long-wavelength helimagnetic order and skyrmion lattice phase in Cu_2OSeO_3," Phys. Rev. Lett. **108**, 237204 (2012).

[12] S. Seki, J.-H. Kim, D. S. Inosov, R. Georgii, B. Keimer, S. Ishiwata, and Y. Tokura, "Formation and rotation of skyrmion crystal in the chiral-lattice insulator Cu_2OSeO_3," Phys. Rev. B **85**, 220406 (2012).

[13] J. H. Yang, Z. L. Li, X. Z. Lu, M.-H. Whangbo, S.-H. Wei, X. G. Gong, and H. J. Xiang, "Strong Dzyaloshinskii-Moriya interaction and origin of ferroelectricity in Cu_2OSeO_3," Phys. Rev. Lett. **109**, 107203 (2012).

[14] S. L. Zhang, G. v. d. Laan, and T. Hesjedal, "Direct experimental determination of the topological winding number of skyrmions in Cu_2OSeO_3," Nature Communications **8**, 14619 (2017).

[15] L. C. Chapon, P. Manuel, P. G. Radaelli, C. Benson, L. Perrott, S. Ansell, N. J. Rhodes, D. Raspino, D. Duxbury, E. Spill, and J. Norris, "Wish: The new powder and single crystal magnetic diffractometer on the second target station," Neutron News **22**, 22–25 (2011).

[16] O. Arnold, J. Bilheux, J. Borreguero, A. Buts, S. Campbell, L. Chapon, M. Doucet, N. Draper, R. F. Leal, M. Gigg, V. Lynch, A. Markvardsen, D. Mikkelson, R. Mikkelson, R. Miller, K. Palmen, P. Parker, G. Passos, T. Perring, P. Peterson, S. Ren, M. Reuter, A. Savici, J. Taylor, R. Taylor, R. Tolchenov, W. Zhou, and J. Zikovsky, "Mantid–data analysis and visualization package for neutron scattering and μ SR experiments," Nucl. Instrum. Methods Phys. Res. A **764**, 156–166 (2014).

[17] J. Rodríguez-Carvajal, "Recent advances in magnetic structure determination by neutron powder diffraction," Physica B Condens. Matter **192**, 55–69 (1993).

[18] A. Bauer and C. Pfleiderer, "Magnetic phase diagram of MnSi inferred from magnetization and ac susceptibility," Phys. Rev. B **85**, 214418 (2012).

[19] A. Bauer and C. Pfleiderer, "Generic aspects of skyrmion lattices in chiral magnets," in *Topological Structures in Ferroic Materials*, edited by J. Seidel (Springer International Publishing, Cham, 2016), Vol. 228, pp. 1–28.

[20] C. Kittel, *Introduction to Solid State Physics*, 7th ed. (Wiley, Hoboken, NJ, 1996).

[21] M. C. Langner, S. Roy, S. K. Mishra, J. C. T. Lee, X. W. Shi, M. A. Hossain, Y.-D. Chuang, S. Seki, Y. Tokura, S. D. Kevan, and R. W. Schoenlein, "Coupled skyrmion sublattices in Cu_2OSeO_3," Phys. Rev. Lett. **112**, 167202 (2014).

[22] S. L. Zhang, A. Bauer, H. Berger, C. Pfleiderer, G. van der Laan, and T. Hesjedal, "Resonant elastic x-ray scattering from the skyrmion lattice in Cu_2OSeO_3," Phys. Rev. B **93**, 214420 (2016).

[23] V. E. Dmitrienko and V. A. Chizhikov, "Weak antiferromagnetic ordering induced by Dzyaloshinskii-Moriya interaction and pure magnetic reflections in MnSi-type crystals," Phys. Rev. Lett. **108**, 187203 (2012).

[24] V. A. Chizhikov and V. E. Dmitrienko, "Microscopic description of twisted magnet Cu_2OSeO_3," Journal of Magnetism and Magnetic Materials **382**, 142–151 (2015).